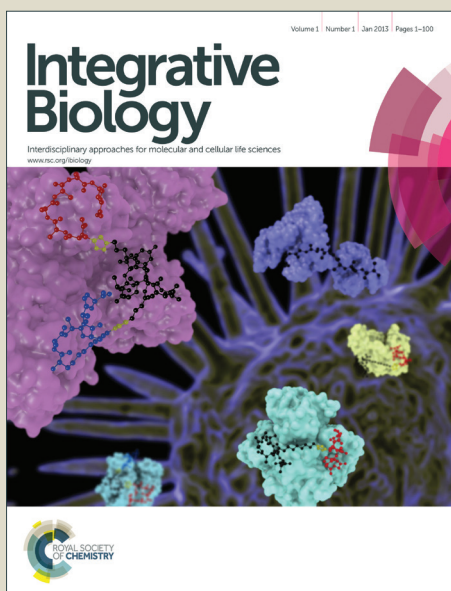


Integrative Biology

Accepted Manuscript



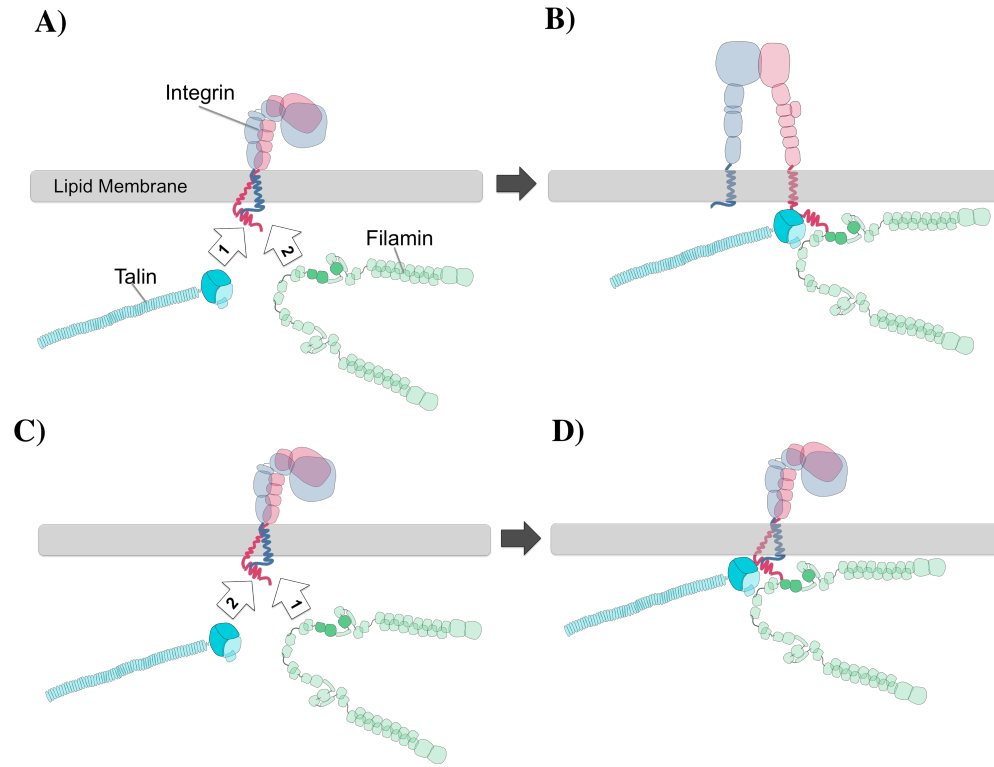
This is an *Accepted Manuscript*, which has been through the Royal Society of Chemistry peer review process and has been accepted for publication.

Accepted Manuscripts are published online shortly after acceptance, before technical editing, formatting and proof reading. Using this free service, authors can make their results available to the community, in citable form, before we publish the edited article. We will replace this *Accepted Manuscript* with the edited and formatted *Advance Article* as soon as it is available.

You can find more information about *Accepted Manuscripts* in the [Information for Authors](#).

Please note that technical editing may introduce minor changes to the text and/or graphics, which may alter content. The journal's standard [Terms & Conditions](#) and the [Ethical guidelines](#) still apply. In no event shall the Royal Society of Chemistry be held responsible for any errors or omissions in this *Accepted Manuscript* or any consequences arising from the use of any information it contains.

Mechanisms of the interplay among filamin, integrin and talin during early focal adhesion formation were explored using molecular dynamics simulations.



Bookmark not defined.

Error!

IB-ART-05-2015-000133 - Mechanisms of Integrin and Filamin Binding and Their Interplay with Talin during Early Focal Adhesion Formation

This study seeks to characterize interactions between integrin and focal adhesion protein filamin and examines their interplay with talin. We shed light on the regulation of the integrin-filamin interaction, and explore the potential scenarios for the interplay of integrin and filamin. Moreover, we study the effect of talin on the filamin-integrin interaction and examine possible scenarios that mediate the interplay of these molecules.

Mechanisms of Integrin and Filamin Binding and Their Interplay with Talin during Early Focal Adhesion Formation

Tiffany Truong¹, Hengameh Shams¹, Mohammad Mofrad*

Department of Bioengineering, University of California, Berkeley, CA 94704, USA

¹These authors contributed equally to this work and share the primary authorship.

*Corresponding Author
Mohammad R. K. Mofrad, PhD
Professor, Department of Bioengineering
University of California Berkeley
208A Stanley Hall #1762
Berkeley, CA 94720-1762
Phone: (510) 643-8165
Fax: (510) 642-5835
Email: mofrad@berkeley.edu
<http://biomechanics.berkeley.edu>

Abstract

Filamin plays a key role in cellular biomechanics as an actin cross-linker and as a versatile focal adhesion binding partner. It binds directly to integrins, a family of mechanosensitive transmembrane receptors that mediate attachment to several extracellular ligands such as fibronectin, collagen, and laminin. Filamin binds β -integrin at its cytoplasmic tail, competing with talin, a major integrin activator that plays a chief role in cell adhesion. Herein, we develop molecular dynamics models to study the mechanism of early binding of $\alpha_{\text{IIb}}\beta_3$ integrin with filamin A (FLNa). Our models predict three important electrostatic interactions and one stabilizing hydrophobic interaction that mediate binding between filamin and integrin. In its native conformation, filamin's integrin binding site is auto-inhibited. Our models help shed light on the role of integrin binding on regulating filamin activation. Finally, the effect of talin on the filamin-integrin interaction is explored and possible scenarios of the interplay among these molecules are examined.

Introduction

The cytosolic protein filamin plays a key role in regulating cellular structure, adhesion and motility by crosslinking actin filaments into the three-dimensional orthogonal networks of the cytoskeleton. In addition, filamin plays a crucial regulatory role in cell shape and motility by interacting with over 90 diverse proteins including channels, transmembrane receptors, and transcription factors¹⁻³. One such binding partner is the transmembrane $\alpha\beta$ heterodimer integrin, which is a versatile signal transducer. Integrins transmit mechanical forces bi-directionally while linking extracellular matrix proteins to the focal adhesion machinery.

Genetic defects in filamin often have acute congenital consequences. For example, mutations in filamin A (FLNa) can lead to a wide range of abnormalities in neural and cardiovascular development. Periventricular heterotopia is a X-chromosome-linked disease caused by a mutation in FLNa that hinders neuronal migration during development and to instead collect along the lateral ventricle. Interesting reports of variability in this disease evoke the question of what mechanisms determine its pathogenesis². Understanding filamin's interaction partners and their role in the cell is therefore key to understanding the cellular function in health and disease.

Filamin influences cellular adhesion via a variety of pathways. While filamin is indirectly required for vimentin-mediated integrin recycling to the cell membrane, thereby increasing integrin expression on the cell surface and promoting cell adhesion and spreading^{4,5}, the direct interaction of filamin with integrin is mediated through multiple integrin binding sites on various domains of filamin, facilitating integrin clustering⁶. These versatile functions of filamin can also be important determinants of inside-out integrin-mediated signaling that plays a critical role in both cell adhesion and motility.

Filamin is a V-shaped homodimer with 24 Ig-like repeated domains, two hinge regions, one dimerization domain, and one actin binding domain on each monomer (see **Figure 1**). The actin binding domain (ABD), composed of two calponin homology domains, is situated at the N-terminal, followed by 15 repeated Ig-like domains in a linear structure, a hinge domain, and Ig-like repeats (16 to 23), which are arranged compactly in a paired structure. Repeat 23 is succeeded by a second hinge region and the last Ig-like domain, IgFLN24, which functions as the dimerization domain at the C-terminal of each monomer^{7,8}. The filamin family contains three human isoforms, the most abundant of which is filamin A (FLNa), ubiquitously found in all cell types. In all filamin isoforms, immunoglobulin-like repeat 21 (IgFLNa21) binds most strongly to integrin and is typically considered the main integrin binding site⁹. However, sequence homology comparisons and NMR studies suggest that IgFLNa21 is part of a subgroup of filamin repeats that all bind integrin and similar ligands (e.g. GP1b α and migfilin)⁶. This subgroup of filamin repeats include IgFLN domains 4, 9, 12, 17, 19, 21, and 23⁶. In IgFLNa21, the ligand binding site is the CD face composed of two β strands, which is auto-inhibited by the first β strand of IgFLNa20^{9,10}.

The crystal structure of IgFLNa21 bound to β_7 integrin, and the observations in several experimental studies suggest that auto-inhibition of IgFLNa21 by IgFLNa20 can be regulated via several pathways including alternative splicing of filamin, phosphorylation of both integrin and filamin, and also mechanical forces applied to filamin⁹⁻¹¹. IgFLNa20-21 exhibits a precisely tuned mechanosensitivity to gradual increases in force. The auto-inhibitory IgFLNa20 is first separated from the cryptic binding site on IgFLNa21 at 2-5 pN forces, and then IgFLNa20 and IgFLNa21 unravel when exposed to larger mechanical forces^{12,13}. The removal of auto-inhibition via relatively small forces is sufficient to elicit a substantial (as much as 17-folds) increase in its

affinity for binding of mechanosensitive transmembrane ligands including glycoprotein Ib (GPIb)¹³. This interesting property enables filamin to fulfill its role as a sensitive mechanotransducer positioned on the force-transmitting webs of actin and at the highly interactive focal adhesion. Filamin also binds several other members of the integrin family including β_{1A} , β_{1D} , β_2 , and β_3 integrins¹⁴.

At the focal adhesion site, filamin competes with talin, the central integrin activator, for an overlapping binding site on integrin, with potential negative modulation of integrin activation^{9,15}. Talin binds the membrane distal segment of integrin's β_3 cytoplasmic tail at ⁷³⁹WDTANNPLYDEA⁷⁵⁰, which provides the site of the initial interaction between talin and integrin¹⁶. The activation of integrin by talin is mediated by a subsequent interaction at the more membrane proximal (MP) region of the integrin tail which may unclasp the constituent subunits of integrin^{17,18}. However, disruption of talin's first interaction with the membrane distal portion can inhibit integrin activation as well as a disrupted second interaction with the membrane proximal (MP) portion of integrin¹⁸. The competition of filamin against talin's first interaction with integrin at its membrane distal end could be a protective mechanism for regulating adhesion in response to mechanical forces. However, the mechanism of filamin and talin competition is not yet clear.

In this study, we use molecular modeling to examine the interaction and binding of IgFLNa21 to $\alpha_{IIb}\beta_3$ integrin, highlighting possible mechanisms of early dynamics including various protein-protein interactions and the sequence in which they occur. In addition, we predict the potential effect of the IgFLNa20 auto-inhibitory strand on integrin binding by comparing the interactions between integrin and filamin in the presence and absence of the auto-inhibitory strand. Moreover, we postulate a plausible role for integrin in releasing filamin from

its auto-inhibitory configuration. Finally, we study the effect of talin on the filamin-integrin interaction and explore possible scenarios of the interplay among these molecules.

Recent studies have extensively explored the mechanism of inside-out activation of integrin by talin using molecular dynamics (MD) to model the conformational changes and interactions, which lead to full activation of integrin^{19,20}. Here we focus on the localization of talin and filamin to adhesion sites and their interactions prior to previously described mechanisms of integrin activation once the ligands have already been bound. Our results suggest that the order of binding events at the integrin β_3 tail is a key factor in regulating integrin activation.

Results

The IgFLNa21 CD face Binding to integrin

Integrin signaling is regulated via various interactions at integrin's cytoplasmic tail in a mechanosensitive manner. Talin is a key player in integrin activation and its interplay with other focal adhesion molecules controls further downstream events^{21,22}. It has previously been proposed that filamin binding to the β integrin tail prevents adhesion formation via blocking talin association to integrin⁹, however the molecular mechanism of such competition is not yet clear. Furthermore, the auto-inhibited state of filamin shows a low affinity for integrin and needs to become activated either through mechanical or chemical cues prior to effective engagement with integrin^{10,11}. In this study, we explored the molecular mechanism of integrin binding to filamin in both auto-inhibited and activated states. Using all-atom molecular dynamics (MD) models we investigated the competition between talin and filamin at the β_3 integrin tail during early stages of adhesion formation.

While the energy of salt bridges are usually overestimated in standard MD force fields²³, some MD force fields including CHARMM22 and CHARMM27 are able to provide sufficient accuracy compared to experimental studies²⁴. Furthermore, here we are mostly interested in comparing either different configurations of proteins complexes or different states of a molecule, e.g. inhibited versus activated filamin, and thus relative energies signify more than the absolute values. Also, since molecular dynamics simulations are stochastic in nature and average values are more meaningful, all reported energies are computed averages from simulations.

The Activated conformation of Filamin Binding to Integrin

Analysis of the molecular dynamics trajectories of β_3 integrin and uninhibited IgFLNa21 binding revealed an early hydrophobic anchorage as Ile⁷⁵⁷ on β_3 integrin inserted itself into the exposed hydrophobic pocket on the surface of FLNa21 formed by Leu²²⁷¹ and Phe²²⁸⁵, which appeared to be critical for stable binding between the molecules (**Figure 2A**). This result matched a previously reported insertion of Ile⁷⁸² on β_7 integrin into the same FLNa21 hydrophobic pocket⁹. This interaction stabilizes the orientation that permits the two surfaces to have the most favorable contact by bringing together the cores of each binding region. Other simulations in which integrin and filamin fail to bind do not establish this hydrophobic contact and consequently separate even when a strong electrostatic contact is initially created. We believe that this stability is generated by the key positioning of Ile⁷⁵⁷ not only between the C and D strands of the CD face, but also between its proximal and distal attachments. Its function as a fastener for the appropriate binding arrangement is consequently necessary for the stability required to secure a tight bind in the likely event that integrin and filamin do not optimally position themselves before they interact. The hydrophobic insertion of an Ile into the CD strands of IgFLNa21 is also conserved in β_7 integrin and in IgFLNa20¹⁰. We have shown that it is also conserved in β_3 integrin and appears to be an important component of ligand binding to the CD face of IgFLNa21.

This hydrophobic contact happened within the first nanosecond, allowing strong electrostatic interactions to happen more stably shortly thereafter. Specifically, the securing of the two binding faces together, resulting from the previously mentioned hydrophobic contact, brought Arg⁷⁶⁰ within the vicinity of Asp²²⁸⁷, forming a strong salt bridge at the MD end of integrin's β tail (**Figure 2B**). Afterward, a second salt bridge formed closer to the membrane proximal end of β integrin when Lys⁷⁴⁸ and Glu²²⁷⁶ bind, which secured the two proteins together

at both ends of filamin's CD face (**Figure 2B**). Prior to the formation of this second salt bridge, a transient electrostatic interaction occurred between Glu⁷⁴⁹ and Lys²²⁸⁰ from 2 ns to 6 ns, which helped to bring the C-terminal end of FLNa21 strand C towards β_3 integrin. These two salt bridges that form at the membrane proximal end competed with one another since IgFNA21 must change its orientation in order to bind either Lys⁷⁴⁸ or Glu⁷⁴⁹. Although both residues do bind within the course of our 30 ns total simulations, the salt bridge between Glu⁷⁴⁹ and Lys²²⁸⁰ was of a more transient nature. On the other hand, Lys⁷⁴⁸ and Glu²²⁷⁶ almost always interacted after the aforementioned salt bridge dissociates, but their interaction was unstable and shifted between high and low energy states. We conclude that the binding between integrin and filamin is likely to be stronger and more stable at the membrane distal end of the integrin tail while it is weaker and less stable at the membrane proximal end. The average simulated energies for the four specific interactions mentioned above were calculated from the ten trials and reported in **Table 1**.

As illustrated in **Figure 2C**, the average interaction energy between β_3 integrin and FLNa taken among 10 trials, became more stable after 8 ns when salt bridges were formed. Although the electrostatic interactions contributed more to the total interaction energy and were quantitatively stronger, they were relatively transient compared to the first hydrophobic interaction that lasted during the entire length of the simulations. In other trials where electrostatic interactions formed without the hydrophobic pocket interaction, the overall energy tended to dissipate over time as molecules did not display high surface contacts.

The α_{IIB} subunit of integrin did not show any direct interaction with filamin in our model, and the interface between α_{IIB} integrin and β_3 integrin remained stable throughout the progression of filamin binding to β_3 integrin as assessed by stable interaction energies at the

inner membrane clasp (IMC). Since the inactive conformation of integrin was used in our simulations, we confirmed that integrin activation was not required for filamin binding⁹.

In the next step, we predicted the major interactions and their relative contributions to filamin and integrin binding. Our simulations suggested that three progressive interactions are important for IgFLNa21 binding to the cytoplasmic tail of β integrin: 1) First, a hydrophobic insertion of Ile⁷⁵⁷ at the center of the CD face of filamin; 2) second, a strong salt bridge at the membrane distal end of integrin between Arg⁷⁶⁰ and Asp²²⁸⁷; 3) finally, a weaker salt bridge at the more membrane proximal end of integrin between Lys⁷⁴⁸ and Glu²²⁷⁶. Our results also confirmed that filamin binding neither activated integrin nor required integrin activation at any stage as was previously shown⁹. This was verified by the stability of integrin's IMC interaction throughout the entire simulation. To our knowledge, these important interactions required for the successful binding between filamin and integrin have not been previously reported.

The Auto-inhibitory Strand of Filamin Binding to Integrin

Filamin is known to regulate its binding to integrin at IgFLNa21 via a self inhibitory interaction between the first strand of IgFLNa20 with the CD face of IgFLNa21, which is the binding site for the β tail of integrin¹⁰. The interaction between the auto-inhibited state of IgFLNa19-21 and integrin was explored in two different orientations of filamin with respect to the integrin tail. In the first model (Model 1), the inhibited IgFLNa21 CD face was placed in proximity to the filamin-binding site on integrin as determined by the presence of Ile⁷⁵⁷ (**Figure 3A**), while in the second model (Model 2), it faced residues on the opposite surface of the integrin tail (**Figure 3B**). These two orientations were modeled to assess the affinity of filamin in its auto-inhibited state to integrin while positioned with and without resemblance to its

orientation when bound in its active state. The results showed that of the overall ten trials with β_3 integrin in the presence of auto-inhibited filamin, five exhibited a fairly stable binding between filamin and integrin. Four of the five successful trials were derived from Model 2 and interactions were consistently stronger in Model 2 compared to Model 1 (**Figure 3**).

In reference to the strength of the interactions we observed in these models, Model 2 exhibited stronger interactions between filamin and integrin and demonstrated a stable interaction. In this model, the integrin β tail interacted at average energies reaching -103 kcal/mol at the auto-inhibitory strand and reaching -67 kcal/mol at the inhibited IgFLNa21 CD face (see **Supplementary Table S1**). The average energy of interaction between integrin and filamin in trials that exhibited binding at these regions was -54 ± 18 kcal/mol at the CD face and -57 ± 29 kcal/mol at the auto-inhibitory strand. In addition, twice as many trials exhibited binding of integrin with the auto-inhibitory strand versus with the CD face beneath it. As such, interactions between integrin and auto-inhibited filamin seem to be achievable even at the covered CD face, but could occur with greater strength and likelihood with the auto-inhibitory strand itself.

Model 1 demonstrated infrequent interaction between integrin and filamin in its auto-inhibited state. Only one trial demonstrated any interaction, which occurred most strongly between Glu⁷⁴⁹ on integrin and Arg²¹³⁹ on the auto-inhibitory strand. Of note, the configuration of both molecules during this interaction resembled the orientation of binding between uninhibited filamin and integrin. That is, the more membrane proximal portion of integrin binds the turn connecting the C and D strands of IgFLNa21. Occasionally, there were also interactions between Arg⁷⁶⁰ and Glu⁷⁴⁹ (**Supplementary Figure S1**).

In contrast, Model 2 exhibited consistent interactions between integrin and filamin in its auto-inhibited state. Two consistently stable interactions were observed: (1) Lys⁷⁴⁸ on integrin engaged with inhibited filamin at two residues on both components of filamin, that is Glu²²⁸² on the CD face and Glu²¹⁴² on the auto-inhibitory strand; (2) Glu⁷⁴⁹ on integrin interacted weakly with a highly basic region on the auto-inhibitory strand consisting of three arginine residues, Arg²¹⁴⁶⁻²¹⁴⁸. These interactions are depicted in (**Supplementary Figure S1**).

From our MD simulations, we predicted that filamin in its auto-inhibited state may interact with integrin in a stable manner at a position distinct from its conformation during binding in an active state. The responsible residues on integrin were the same ones responsible for the weaker salt bridges formed when integrin binds to filamin in its active state. However, they appeared to bind the auto-inhibitory strand itself, and to a lesser degree the covered CD face of filamin.

A Competition between Filamin and Talin

The competition between talin and filamin for the same binding site on integrin was proposed to be one of the most important regulatory mechanisms for integrin activation⁹, however, the details of their interplay are not yet fully understood. Previous studies showed that increased filamin binding to integrin in Chinese hamster ovary cells inhibited migration¹⁵. On the contrary, the presence of talin is essential for forming nascent adhesions and is found localized to protruding regions of lamellipodium indicative of a major role in cellular motility as well as adhesion^{25,26}. Outcomes concerning integrin functionality including cell migration and adhesion appear then to be regulated by filamin binding^{15,27}, which is complicated by competition with activating ligands such as talin⁹.

In this study, we hypothesized that the order of binding events among integrin, talin and filamin prior to integrin activation is most likely a key factor in promoting subsequent signaling pathways. Specifically, the objective of this study was to understand the early dynamics of possible competitive versus cooperative mechanisms between filamin and talin interactions with the integrin tail, which ultimately localizes them to the adhesion sites. We examined three possible scenarios: 1) In the first scenario, filamin and talin were placed at equal distances away from their binding site on the integrin tail such that none was favored; 2) In the second scenario, talin was placed closer to the integrin (also referred to as the talin-bound simulations) and lastly 3) filamin was moved closer to integrin, while talin was positioned farther away (also referred to as the filamin-bound simulations).

In the first scenario, we investigated the relative likelihood of filamin and talin binding to integrin in a fair competition. Although 5 ns simulation time was not sufficient for the formation of stable interactions, it provided an insight on the primary dynamics of the system. The integrin tail either swung closer to filamin or stayed at the same position in all five trials. Therefore, integrin could engage at least weakly with filamin but not with talin, especially toward the end of simulations.

In order to investigate the interplay between talin and filamin in the second scenario, the native structure of the talin F2 and F3 domains in complex with the β -integrin tail was obtained from the protein data bank (PDB ID: 3G9W)²⁸. The F2 and F3 domains of talin were oriented correctly, based on the crystal structure of the complex, with respect to their binding site on integrin but slightly moved away within the cut-off distance of the non-bonded interactions to allow surface adjustments at the integrin-talin interface. On the other hand, filamin was placed at a farther distance such that it had a lower chance to interact with its binding site on integrin.

All interaction energies observed during the process of integrin activation is signified by a reduction in the interaction between α and β subunits at the cytoplasmic side, and thus talin, as a primary activator of integrin, was expected to weaken the strength of integrin dimerization. The pairwise interaction energy of integrin subunits showed a 50 kcal/mol decrease (**Figure 4A**). The interaction energy between talin and β -integrin, which was averaged over five trials, indicated an oscillatory behavior between 0 and -200kcal/mol suggesting that the presence of filamin reduced the stability of talin-integrin interactions (**Figure 4B**). Talin was bound towards the C-terminal end of β -integrin tail mainly through electrostatic interactions. Also, filamin binding to integrin overlapped with the partial dissociation of integrin subunits in the last 1 ns (**Figure 4C**).

Further analyses of the simulation trajectories of the second scenario showed an interesting prediction of the force transmission dynamics from the point of contact between talin and integrin to the interface between integrin subunits (**Figure 5A**). Specifically, an interaction between TRP⁹⁸⁸ on α -integrin and ILE⁷¹⁹ on β -integrin was replaced by an interaction between TRP⁹⁸⁸ and TRP⁷¹⁵ after around 3 ns, which occurred in response to talin association with the β ₃-integrin tail. The transmembrane helix of β ₃-integrin stretches to the cytoplasm and is connected to a smaller helix (residues 743-750) via a loop region. Initially, the small cytoplasmic α -helix was not fully aligned with its binding site on the F3 domain of talin and GLU³⁷⁵ on the F3 domain was associated with LYS⁷³⁸ on the β -integrin tail. After 2 ns of simulation, LYS⁷³⁸ was released from GLU³⁷⁵ and associated with GLU³⁷⁸, which contributed to the alignment between the small α -helix of integrin and F3 domain of talin leading to formation of new electrostatic interactions (**Figure 5B-E**). Interestingly, filamin engaged with both integrin and

talin simultaneously (**Figure 4C-D**) through one of its residues (VAL²⁵⁵), which formed an interaction with PRO³⁶⁶ on talin after 3 ns. Since filamin bound to the lower segment of integrin tail closer to the C-terminal, we observed that it affected the alignment between the small α -helix on β -integrin and a β -sheet face of the F3 domain of talin (**Figure 5**).

In the third scenario, filamin was positioned at a closer proximity of β -integrin compared to talin such that interactions were more likely to occur between integrin and filamin. Although talin bound to integrin after filamin, the interaction between integrin subunits remained intact (**Figure 4E**). However, the overall interaction energy between integrin subunits was significantly decreased (~ 110 kcal/mol) compared to that in the talin-bound simulations (second scenario shown in **Figure 4A**). In order to understand such energy difference, the final configuration of the integrin dimer in the filamin-bound system was aligned with that in the talin-bound system.

Interestingly, a notable decrease in the angle between integrin subunits, which was initially set at 25° ²⁹ in the filamin-bound system was observed. This angle change resulted in reducing several interactions at the N-terminal of the transmembrane part of the integrin dimer as well as a segment of ectodomain including ASP⁶⁹² and VAL⁶⁹⁶ of α -integrin with ALA⁹⁵⁶ and ILE⁹⁶⁴ of β -integrin, respectively (**Figure 6**). On the other hand, some interactions in both transmembrane and cytoplasmic regions were notably stabilized due to the parallelization of integrin subunits. Therefore, the reduction in the interaction energy is not indicative of integrin activation.

After equilibrating the filamin-bound system, both talin and filamin formed simultaneous interactions with integrin as shown in **Figures 4F and 4G**. Within the first 2 ns, talin maintained a weak but stable interaction with β -integrin, while the energy of filamin-integrin interaction continuously decreased. At approximately 2 ns, the filamin-integrin energy was stabilized, while

the energy of talin-integrin started to decrease around 3 ns. A relatively stable interaction between filamin and talin was also observed. (**Figure 4H**).

In the third scenario, filamin associated with the lower end of the integrin tail, while talin engaged with the same small α -helix in the middle region of the integrin cytoplasmic tail as observed in talin-bound simulations except with a lower energy. Initially, GLY⁷⁶⁰ on β -integrin interacted with SER¹⁰⁰ and ILE²⁴⁰ on the CD face of filamin, however after 3.8 ns an interaction with talin forced the integrin tail to detach and move towards the lipid membrane eventually interacting with PHE²⁴² on the CD face of filamin (**Supplementary Figure S2**).

Generally, our simulations showed that talin bound closer to the inner membrane clasp (IMC) on the integrin tail, while filamin associated with the membrane distal region of the β -integrin and thus did not affect the IMC interaction. Furthermore, the interaction between filamin and talin depended on which one was first bound to the integrin tail.

Discussion

Filamin plays an important structural and mechanotransducing role in the cell, allowing for versatility in cellular shape and motility. The structure of filamin allows for its own regulation of integrin binding by an auto-inhibitory strand on IgFLNa20. At the focal adhesion, filamin competes with talin for binding to integrin. While talin activates integrin, filamin plays an opposite role.

Filamin's interactions with other proteins in the cell could provide a deeper understanding of diseases linked to filamin mutations. For instance, defects in FLNa that result in the disease periventricular nodular heterotopia have led to cases of individuals who present with platelet dysfunctions including thrombocytopenia and hemorrhage with abnormal platelet morphology. This represents a specific situation in which a reduction in FLNa's interactions with transmembrane receptors such as $\alpha_{IIb}\beta_3$ integrin have led to abnormal platelets and impaired interactions between platelets and vessel walls³⁰. By unraveling the mechanism by which integrin and FLNa bind to perform their functions, it may be possible to elucidate the underlying pathophysiology and design novel means for treatment of such disorders. Here we used $\alpha_{IIb}\beta_3$ integrin from platelets in all our simulations.

Prior studies have described binding between filamin and integrin either at equilibrated states in which stable interactions are already formed with filamin or with given various external parameters such as force applied to filamin^{13,31}. In order to elucidate the role of earlier transient interactions, which set the stage for binding filamin, we have developed molecular dynamics models to simulate important initial interactions including the role of filamin's auto-inhibitory strand and its dynamics in relation to talin.

Our results showed that the auto-inhibitory strand on IgFLNa20 engages strongly with IgFLNa21 with average interaction energy of -282 ± 46 kcal/mol preventing it from efficiently binding with the β_3 integrin tail. Beside the mechanism of alternative splicing, removal of this interaction requires mechanical force to be transmitted through the cytoskeleton with or without residue phosphorylation, indicating that the CD face of IgFLNa21 is tightly concealed in filamin's native conformation. In cases where there is insufficient force to expose the CD face of IgFLNa21, it becomes necessary to examine the effect of the auto-inhibitory strand on the interaction between filamin and integrin.

In simulations where IgFLNa21 was inhibited by IgFLNa20, the auto-inhibitory strand did not completely impede interactions between integrin and filamin. Integrin also continued to weakly interact with inhibited filamin, but more with the auto-inhibitory strand than with the partially exposed residues of the IgFLNa21 CD face. As a result, inhibited filamin may be held within the vicinity of a nearby focal adhesion in a weak but stable manner ready to become activated and reinforce adhesions.

It is interesting to note that inhibited filamin interacted with integrin more consistently in an orientation opposite to the actual filamin binding site (Model 2). This signified the increased likelihood that after filamin is released from its auto-inhibition, the filamin binding site will be available on the integrin tail. In order to bind an integrin that has been weakly interacting with in its auto-inhibited state, the uninhibited filamin must either wrap itself around integrin or detach and reorient itself. The potential implications of this relocating process are unknown.

Lad et al. posited that binding between β_7 integrin and filamin is strong enough to overcome the auto-inhibitory interaction with IgFLNa20 and that binding between integrin and filamin is stronger than the auto-inhibition¹⁰. We did not see evidence of greater binding between

β_3 integrin and IgFLNa21 than between IgFLNa20 and IgFLNa21 as the average interaction energy between uninhibited FLNa21 and β_3 integrin was -170 kcal/mol, compared to -282 kcal/mol between FLNa20 and FLNa21. This difference may be attributed to the use of β_3 integrin in our simulations rather than β_7 integrin. In our studies, auto-inhibited filamin exhibited increased interaction energies with integrin within the range of at least one extra electrostatic interaction. Stochastic fluctuations which allowed higher interaction energies at times during our simulations may allow integrin and IgFLNa20 to compete more evenly for IgFLNa21 binding.

In addition, the interaction between integrin and the auto-inhibitory strand itself may be an important first step in removing auto-inhibition altogether and toward uninhibited filamin and integrin binding. There was some evidence for this in the binding preference of auto-inhibited filamin to residues on integrin that orient it to the conformation of uninhibited binding in our simulations. Specifically, one stable interaction between Glu⁷⁴⁹ and Arg²¹³⁹ bound the membrane proximal portion of the integrin β_3 cytoplasmic tail to the region by the turn between the C and D strands of IgFLNa21.

Consequently, we propose a step-wise mechanism for filamin activation through integrin binding: (i) A reduction in the strength of IgFLNa20-IgFLNa21 interaction upon integrin binding to the auto-inhibitory strand; (ii) Complete dissociation of the auto-inhibitory strand in response to cytoskeletal forces; (iii) Association of integrin with the exposed CD face, which prevents it from possible deactivation (**Figure 7**). In other words, integrin binding to the IgFLNa20 inhibitory strand may act as a transient interaction that imposes forces on the inhibitory strand and reduces the strength of association between IgFLNa20 and IgFLNa21. We hypothesize that this interaction will then be coupled with the forces coming from the cytoskeleton, giving rise to

filamin activation and reinforcement of integrin binding. In our simulations, we did not involve cytoskeletal forces due to the complexity of incorporating the dynamics of such forces in the process of a binding event. Instead, we used both the activated and inhibited segments of filamin in two independent simulations. Hence, we did not observe full activation of filamin due to the lack of cytoskeletal forces but an energy analysis predicted that integrin interaction indeed lowers the energy barrier needed to expose the CD face of IgFLNa21.

Chen, Kolahi et al. proposed that filamin binding to integrin was highly modifiable through a phosphorylation mechanism¹¹. Here, the idea of filamin's role as a "tunable mechanosensor"² was extended to also include interactions with IgFLNa20. Stable interactions between integrin and the IgFLNa20 auto-inhibitory strand suggested that filamin had some affinity for integrin constitutively, whether or not it senses a force through the cytoskeleton. This fits into a mechanoprotective role for filamin binding to integrin to regulate adhesion under mechanical stress conditions. Under stress, filamin will uncover its cryptic binding sites easily. However, under no-stress conditions in which steered molecular dynamics are not applied, filamin was predicted to still bind integrin even while auto-inhibited by IgFLNa20.

Interactions between integrin and the auto-inhibitory strand may play other roles as well. Kiema et al. 2006 hypothesized that, in the event of a dysfunctional IgFLNa21, the presence of other filamin repeats which could bind integrin (i.e. IgFLNa19) may be able to partially compensate for its loss of function. Our findings suggest it is possible that integrin's affinity for the auto-inhibitory strand (IgFLNa20) may also partially provide a compensatory mechanism for a defective IgFLNa21. Future studies of filamin's role as an integrin binding partner might explore the effects of auto-inhibitory strand binding in the context of phosphorylation or mechanical force applied to filamin.

Several studies suggested that the interplay among talin and filamin is crucial for regulating integrin activation in migrating cells⁹. As nascent adhesions start to form, talin molecules are recruited, while filamin concentration increases during the maturation stage. Although, talin is the main integrin activator, it may not be required for further cell spreading. Different types of integrin show distinct regulatory mechanisms in their interactions with filamin and talin¹⁵. Here we report important predictions inferred from MD simulations on the order of talin and filamin binding to integrin $\alpha_{\text{IIb}}\beta_3$ and its effect on regulating the dynamics of integrin activation. It should be noted that integrin activation can primarily be characterized by weakening of the linkage between integrin subunits¹⁸.

We compared two different cases in terms of the relative positions of talin and filamin with respect to integrin: (1) In the first case, talin was positioned relatively closer to the β -integrin tail compared to filamin while, (2) in the second case, filamin was put closer to integrin. Comparing the interface between integrin monomers in both cases revealed that major talin association to integrin prior to filamin resulted in destabilizing the interface (**Figure 4A**). However, as shown in **Figure 4C**, talin interaction with integrin was highly fluctuating due to the presence of filamin indicating that filamin interfered with the dynamics of talin-integrin binding. Furthermore, the interaction between filamin and talin increased towards the end of talin-bound simulations that resulted in destabilization of the talin-integrin complex indicating the competition between talin and filamin. On the contrary, in the filamin-bound simulations, the interaction between filamin and talin was formed early on and lasted all throughout the simulations. This suggests that the interaction between filamin and talin may be dependent on the order of their binding to the integrin tail. Furthermore, talin binding is necessary and most likely

sufficient for integrin activation, and consecutive filamin binding may not affect the process of integrin activation only if talin is already bound to integrin.

In the filamin-bound simulations, the interface between integrin subunits was stable but energetically lowered compared to the talin-bound simulations (**Figure 4E**). That was due to an angle change between integrin subunits resulting in the disruption of several interactions mainly within the transmembrane region of integrin subunits. This angle change may act as a lock for further signal transmission across the transmembrane region, and hence the increase in the energy of the integrin dimer in the filamin-bound simulations did not indicate activation but may in fact show functional stabilization of the inactive conformation. Even though talin associated with integrin in the filamin-bound simulations, it did not cause any change at the interface between integrin subunits. Moreover, here we observed that neither the active nor inactive filamin changed the strength of integrin dimerization. Therefore, we predict that filamin may act as an inhibitor of integrin activation when it first binds to integrin regardless of presence or absence of talin.

In order to explore a fair competition between filamin and talin, a set of simulations was designed in which filamin and talin were positioned at the same distance from their binding site on integrin giving both equal chances to engage with integrin. Our results suggested that integrin tail floated towards filamin and even slightly interacted while there was no notable interaction was formed with talin. It should be noted that even though 5 ns of simulations was not long enough for formation of a stable protein complex, it provided a valuable insight on the early dynamics of the competition between talin and filamin in the first few nanoseconds and all reported results were averaged across five trials in order to improve the statistical significance.

Several systems are known to exist with relationships comparable to that of filamin and talin in regards to competition for integrin binding, and there is much variance between the mechanisms and consequences of these systems. Kindlin and talin, for example, have been found to have sequence homology with each other and both bind to integrin β tails, however kindlin and talin are cooperative in effect and are partners in the activation of integrin²². In another example, RIAM and vinculin have also been found to be mutually exclusive by structure in their binding to talin, but unlike filamin versus talin competition for integrin, binding of RIAM versus vinculin appears to occur under more distinguishing circumstances with vinculin binding only unfolded talin domains and RIAM only binding folded talin domains^{32,33}.

In summary, we proposed a mechanism for filamin activation through integrin binding to the auto-inhibitory strand associated with IgFLA21. Also, we predicted that filamin interference with talin-induced integrin activation depends on the sequence of binding events (**Figure 8**). Moreover, our results suggested that the mutual interactions between filamin and talin regulate their competition for integrin binding. Our simulations complement the predictions of previous experimental studies and will hopefully inspire future experimental investigations including testing new mutations involved in the proposed mechanisms.

Materials and Methods

The interaction of filamin with integrin and talin was investigated using molecular dynamics models developed in the software package NAMD³⁴ with CHARMM27 force field³⁵. The structures used here include the transmembrane and cytoplasmic domains of $\alpha_{11b}\beta_3$ integrin (PDB ID: 2K9J), IgFLNa21 (PDB ID: 2BRQ), IgFLNa19-21 (PDB ID: 2J3S) and talin from the talin-integrin complex (PDB ID: 3G9W) All simulations contained a POPC lipid membrane generated by the membrane builder plug-in from the Visual Molecular Dynamics (VMD) package. Proteins were placed a minimum of 10Å apart to avoid steric contacts and solvated using TIP3P explicit water model and the ion concentration was set to 0.15M NaCl. All simulations were linearly heated to 310 K and the temperature was held constant for equilibration as a closed system. An NPT ensemble utilizing Langevin dynamics was applied to hold the pressure at 1 atm. Electrostatic force calculations were made using the particle mesh Ewald (PME) method. Each time step was 2 fs, and the cutoff distance for non-bonded interactions was 1.2 nm. Visualizations were performed using VMD.

Molecular Dynamics of IgFLNa21 CD face and Activated Filamin Binding

To model the dynamics of IgFLNa21 binding to β_3 integrin, one IgFLNa21 molecule was isolated from a crystal structure (PDB ID: 2BRQ) containing two IgFLNa21s bound to two different β_7 integrins. This IgFLNa21 was placed 10 angstroms from the β_3 tail of an $\alpha_{11b}\beta_3$ integrin whose extracellular domains were excised and that was embedded in a POPC lipid membrane.

Seven trials of this model were equilibrated for 20 ns. Successful trials were used to analyze important electrostatic and hydrophobic interactions leading to binding between integrin

and filamin. For the purpose of defining specific hydrophobic interactions within the hydrophobic region of FLNa21, the residues on either side of the inserting Ile⁷⁵⁷ on each strand of the CD face were chosen to represent the hydrophobic pocket.

The interaction between these three residues proved to be the stable core of the hydrophobic insertion, although other hydrophobic residues that make up the CD face surrounding them likely lend strength to the hold on Ile⁷⁵⁷. These neighboring residues include Ala²²⁷², Ile²²⁷³, and Ile²²⁸³.

The activated structure of filamin¹¹, containing repeats 19 to 21, was used to study its interaction with integrin. The initial distance of the activated filamin from integrin was similar to that in the simulation of only repeat 21 binding to integrin. The simulations resulted in strong bound conformation of activated filamin and integrin, which was in turn used in simulations done in the presence of talin (see ‘Filamin and talin competition in integrin binding’ in **Materials and Methods**).

The final bound structure resulting from the end of the successful trial was used for ten more simulations. Each of these simulations involved reheating to 310 K in order to randomize velocities and then an equilibration step for 10 ns. From the last 10 ns, average energies of interaction were calculated for the final bound structure of IgFLNa21 with β_3 integrin.

The IgFLNa20 Auto-inhibitory Strand

Two models were created by placing the crystal structure of IgFLNa19-21 (PDB ID: 2J3S) 10Å away from two different sides of the backbone of the β_3 integrin tail. The cut $\alpha_{11b}\beta_3$ integrin was placed in a POPC lipid membrane. Five trials of each model were heated linearly to 310 K to randomize molecular velocities and then equilibrated for 13 ns each. Average energies

of interaction were calculated from the last 8 ns of all ten trials, and from all trials from each model alone. The first 5 ns were left out in order to account for a period of minimization and equilibration.

Filamin and Talin Competition in Integrin Binding

In this phase of the study, talin was also included in simulations and positioned in various distances from filamin and integrin. Since the crystal structure of talin is not entirely available, only the F2 and F3 domains that contain the integrin binding site were used in our simulations²⁸ (PBD ID: 3G9W). The regions of integrin and filamin used in this part were similar to the previous parts of this study.

Three simulation sets with five trials were performed for 5 ns in order to examine the role of talin in filamin-integrin interaction. In the first set, both talin and filamin were positioned at distances larger than the cut-off range for non-bonded interactions relative to integrin (the closest atoms were farther away than 15 Å). In the second set, talin was positioned in the vicinity of the filamin-integrin complex found from the previous simulations (see ‘Molecular Dynamics of IgFLNa21 CD face and Activated Filamin Binding’ in **Materials and Methods**). In the third set, the available structure of the talin was put in complex with integrin, while filamin was positioned away from its binding site on integrin²⁸. All simulations were minimized and equilibrated prior to the production run. The condition for temperature, pressure and ion concentration was the same as the previous simulations. Although the simulation box changed for each system according to the system size, all satisfied the minimum image convention by setting the minimum distance between the salute and wall to be greater than 22 Å.

Upon completion of all simulations, the following pairwise energies were calculated and averaged among 5 trials: 1) Integrin subunits; 2) β -Integrin and filamin, 3) β -Integrin and talin; 4) α -Integrin and filamin; 5) α -Integrin and talin; And also 6) mutual interaction between filamin and talin. Also, all important residues participating in the above interactions were analyzed and discussed.

Acknowledgments

Financial support by a National Science Foundation CAREER award (CBET-0955291) is gratefully acknowledged. We appreciate fruitful discussions with Mehrdad Mehrbod and other members of the Molecular Cell Biomechanics Laboratory. This research used resources of the National Energy Research Scientific Computing Center, a DOE Office of Science User Facility supported by the Office of Science of the U.S. Department of Energy under Contract No. DE-AC02-05CH11231. Also, This work used the Extreme Science and Engineering Discovery Environment (XSEDE), which is supported by National Science Foundation grant number ACI-1053575.

References

- 1 L. J. Sampson, M. L. Leyland and C. Dart, *J. Biol. Chem.*, 2003, **278**, 41988–97.
- 2 Y. Feng and C. A. Walsh, *Nat. Cell Biol.*, 2004, **6**, 1034–8.
- 3 G. M. Popowicz, M. Schleicher, A. A. Noegel and T. A. Holak, *Trends Biochem. Sci.*, 2006, **31**, 411–9.
- 4 H. Kim, F. Nakamura, W. Lee, C. Hong, D. Pérez-Sala and C. A. McCulloch, *Exp. Cell Res.*, 2010, **316**, 1829–44.
- 5 H. Kim, F. Nakamura, W. Lee, Y. Shifrin, P. Arora and C. A. McCulloch, *Am. J. Physiol. Cell Physiol.*, 2010, **298**, C221–36.
- 6 S. S. Ithychanda, D. Hsu, H. Li, L. Yan, D. D. Liu, D. Liu, M. Das, E. F. Plow and J. Qin, *J. Biol. Chem.*, 2009, **284**, 35113–21.
- 7 R. Pudas, T.-R. Kiema, P. J. G. Butler, M. Stewart and J. Ylänne, *Structure*, 2005, **13**, 111–9.
- 8 B. a Kesner, S. L. Milgram, B. R. S. Temple and N. V Dokholyan, *Mol. Biol. Evol.*, 2010, **27**, 283–95.
- 9 T. Kiema, Y. Lad, P. Jiang, C. L. Oxley, M. Baldassarre, K. L. Wegener, I. D. Campbell, J. Ylänne and D. A. Calderwood, *Mol. Cell*, 2006, **21**, 337–47.
- 10 Y. Lad, T. Kiema, P. Jiang, O. T. Pentikäinen, C. H. Coles, I. D. Campbell, D. A. Calderwood and J. Ylänne, *EMBO J.*, 2007, **26**, 3993–4004.
- 11 H. S. Chen, K. S. Kolahi and M. R. K. Mofrad, *Biophys. J.*, 2009, **97**, 3095–104.
- 12 H. Chen, S. Chandrasekar, M. P. Sheetz, T. P. Stossel, F. Nakamura and J. Yan, *Sci. Rep.*, 2013, **3**, 1642.
- 13 L. Rognoni, J. Stigler, B. Pelz, J. Ylänne and M. Rief, *Proc. Natl. Acad. Sci. U. S. A.*, 2012, **109**, 19679–84.
- 14 T. P. Stossel, J. Condeelis, L. Cooley, J. H. Hartwig, A. Noegel, M. Schleicher and S. S. Shapiro, *Nat. Rev. Mol. Cell Biol.*, 2001, **2**, 138–45.
- 15 D. A. Calderwood, A. Huttenlocher, W. B. Kiosses, D. M. Rose, D. G. Woodside, M. A. Schwartz and M. H. Ginsberg, *Nat. Cell Biol.*, 2001, **3**, 1060–8.
- 16 B. García-Alvarez, J. M. de Pereda, D. A. Calderwood, T. S. Ulmer, D. Critchley, I. D. Campbell, M. H. Ginsberg and R. C. Liddington, *Mol. Cell*, 2003, **11**, 49–58.
- 17 O. Vinogradova, A. Velyvis, A. Velyviene, B. Hu, T. A. Haas, E. F. Plow and J. Qin, *Cell*, 2002, **110**, 587–597.
- 18 K. L. Wegener, A. W. Partridge, J. Han, A. R. Pickford, R. C. Liddington, M. H. Ginsberg and I. D. Campbell, *Cell*, 2007, **128**, 171–82.
- 19 D. Provasi, A. Negri, B. S. Collier and M. Filizola, *Proteins*, 2014, **82**, 3231–40.
- 20 A. C. Kalli, I. D. Campbell and M. S. P. Sansom, *Proc. Natl. Acad. Sci. U. S. A.*, 2011, **108**, 11890–5.

- 21 B. G. Petrich, P. Marchese, Z. M. Ruggeri, S. Spiess, R. A. M. Weichert, F. Ye, R. Tiedt, R. C. Skoda, S. J. Monkley, D. R. Critchley and M. H. Ginsberg, *J. Exp. Med.*, 2007, **204**, 3103–11.
- 22 F. Ye, F. Lagarrigue and M. H. Ginsberg, *Cell*, 2014, **156**, 1340–1340.e1.
- 23 K. T. Debiec, A. M. Gronenborn and L. T. Chong, *J. Phys. Chem. B*, 2014, **118**, 6561–9.
- 24 S. Piana, K. Lindorff-Larsen and D. E. Shaw, *Biophys. J.*, 2011, **100**, L47–9.
- 25 R. Zaidel-Bar, C. Ballestrem, Z. Kam and B. Geiger, *J. Cell Sci.*, 2003, **116**, 4605–13.
- 26 C. Lawson, S.-T. Lim, S. Uryu, X. L. Chen, D. A. Calderwood and D. D. Schlaepfer, *J. Cell Biol.*, 2012, **196**, 223–32.
- 27 J. Liu, M. Das, J. Yang, S. S. Ithychanda, V. P. Yakubenko, E. F. Plow and J. Qin, *Nat. Struct. Mol. Biol.*, 2015, **22**, 383–389.
- 28 N. J. Anthis, K. L. Wegener, F. Ye, C. Kim, B. T. Goult, E. D. Lowe, I. Vakonakis, N. Bate, D. R. Critchley, M. H. Ginsberg and I. D. Campbell, *EMBO J.*, 2009, **28**, 3623–32.
- 29 F. Ye, A. K. Snider and M. H. Ginsberg, *Front. Med.*, 2014, **8**, 6–16.
- 30 P. Nurden, N. Debili, I. Coupry, M. Bryckaert, I. Youlyouz-Marfak, G. Solé, A.-C. Pons, E. Berrou, F. Adam, A. Kauskot, J.-M. D. Lamazière, P. Rameau, P. Fergelot, C. Rooryck, D. Cailley, B. Arveiler, D. Lacombe, W. Vainchenker, A. Nurden and C. Goizet, *Blood*, 2011, **118**, 5928–37.
- 31 U. Pentikäinen and J. Yläne, *J. Mol. Biol.*, 2009, **393**, 644–57.
- 32 D. A. Calderwood, I. D. Campbell and D. R. Critchley, *Nat. Rev. Mol. Cell Biol.*, 2013, **14**, 503–17.
- 33 B. T. Goult, T. Zacharchenko, N. Bate, R. Tsang, F. Hey, A. R. Gingras, P. R. Elliott, G. C. K. Roberts, C. Ballestrem, D. R. Critchley and I. L. Barsukov, *J. Biol. Chem.*, 2013, **288**, 8238–49.
- 34 J. C. Phillips, R. Braun, W. Wang, J. Gumbart, E. Tajkhorshid, E. Villa, C. Chipot, R. D. Skeel, L. Kalé and K. Schulten, *J. Comput. Chem.*, 2005, **26**, 1781–802.
- 35 A. D. MacKerell, D. Bashford, R. L. Dunbrack, J. D. Evanseck, M. J. Field, S. Fischer, J. Gao, H. Guo, S. Ha, D. Joseph-McCarthy, L. Kuchnir, K. Kuczera, F. T. K. Lau, C. Mattos, S. Michnick, T. Ngo, D. T. Nguyen, B. Prodhom, W. E. Reiher, B. Roux, M. Schlenkrich, J. C. Smith, R. Stote, J. Straub, M. Watanabe, J. Wiórkiewicz-Kuczera, D. Yin and M. Karplus, *J. Phys. Chem. B*, 1998, **102**, 3586–3616.

Figure Legends:

Figure 1. Schematics of filamin interaction with actin filaments. Each filamin monomer consists of 24 Ig repeats and two hinge regions between repeats 16-17 and 23-24. The actin binding domain (ABD) is located at the N-terminal end, while the main integrin binding sites (IBS) are on repeats 19 and 21 that are auto-inhibited by repeat 20. Filamin monomers dimerize through their last Ig repeat.

Figure 2 – Interactions between uninhibited filamin and β_3 integrin **A)** The model depicts FLNa21 CD strands (*green*) and β_3 integrin (*red*) backbones in ribbon representation. At 1 ns, the two proteins began to interact when Ile⁷⁵⁷ on β_3 integrin inserted into the hydrophobic pocket formed by Leu²²⁷¹ and Phe²²⁸⁵. This hydrophobic interaction stabilizes the binding between integrin and filamin by promoting high surface contacts. **B)** Arg⁷⁶⁰ formed a strong, persistent salt bridge with Asp²²⁸⁷ that accounted for most of the strength of binding between integrin and filamin around 2 ns and lasted until the end of simulation (snapshot shown here). Another salt bridge formed between Lys⁷⁴⁸ and Glu²²⁷⁶ closer to the MP end of β_3 . **C)** The interaction energy between β_3 integrin and uninhibited IgFLNa21 was averaged across ten trials of reheating and equilibration for 10 ns. The average energy of the electrostatic interactions accounted for most of the strength of binding.

Figure 3 – Two models were created to simulate a randomized encounter between inhibited filamin containing IgFLNa20-21 and β_3 integrin. **A)** The first orientation placed the inhibited FLNa21 CD face on the side of integrin that is favorable for binding when uninhibited. It faced the residues on integrin that typically interact with the filamin CD face. As expected, the energy of interaction was negligible indicating that inhibited filamin did not have a tendency to bind to the standard filamin binding site on β_3 integrin. **B)** The second orientation placed the inhibited FLNa21 CD face opposite to the side of integrin that is favorable for uninhibited binding. It faced different residues than those that typically interact with the filamin CD face. The interaction energy showed a relatively strong association between inhibited filamin and β_3 integrin.

Figure 4 – A comparison between talin-bound and filamin-bound simulations: Electrostatic (*red*), van der Waals (*blue*) and total energies (*black*) are shown. **Talin-bound simulations:** **A)** The total interaction energy of integrin subunits shows a 50 kcal/mol increase starting around 3.2 ns. **B)** Talin interaction with β_3 -integrin demonstrated an oscillatory behavior. **C)** Filamin weakly interacted with β_3 -integrin in the first half of simulations but dissociated in the second half. **D)** Talin-filamin interaction energy became stronger towards the end of simulations. **Filamin-bound simulations:** **E)** The interaction energy of integrin subunits was constant but got approximately 110 kcal/mol weaker compared to talin-bound simulations. **F)** Talin interaction with β_3 -integrin was much weaker than the case where talin was first bound to integrin, while **G)** filamin-integrin interaction was about five times stronger than talin-bound simulations. **H)** On the contrary to the talin-bound simulations, filamin and talin got engaged since the beginning of simulations.

Figure 5 – A) Talin bound to the more proximal region of integrin tail, while filamin associated with the distal portion of β_3 -integrin (the binding residues are circled). **B)** The dynamics of talin-integrin binding showed that Lys⁷³⁸ acted as an anchor that held talin in place by switching from interacting with GLU375 **C)** to GLU378 at 2 ns in order for the small α -helix of the cytoplasmic side of β_3 -integrin to align with its binding site on the F3 domain of talin (**D, E**).

Figure 6 – Difference in the alignment of integrin monomers between talin-bound and filamin-bound simulations. Integrin subunits form a 25° angle with each other inside the lipid membrane that accounts for the formation of several stable interactions between integrin subunits including ASP⁶⁹² and

VAL⁶⁹⁶ of β_3 -integrin with ALA⁹⁵⁶ and ILE⁹⁶⁴ of α -integrin **A**) This angle was maintained in talin bound simulations, while **B**) it was notably reduced in filamin-bound simulations.

Figure 7 The mechanism of filamin activation through integrin binding. A) Relatively weak interaction between filamin and the auto-inhibitory strand may reduce the strength of inhibitory interactions and also serves as an anchorage point. As actin forces applied on the rod domain of filamin, are transmitted to the complex of auto-inhibitory strand and integrin, it may result in dissociating the auto-inhibitory strand from IgFLNA21 and leave the CD face exposed to water. **B)** Also, since the auto-inhibitory strand binds to the opposite side of the integrin tail relative to the filamin binding site, integrin can subsequently dissociate from the auto-inhibitory strand and engage with the activated filamin on its actual binding site and prevent further deactivation of the molecule.

Figure 8 – Summary of the talin-filamin interplay in integrin activation: A-B) In simulations where talin was associated with the inactive conformation of integrin prior to filamin, the interactions between integrin subunits were weakened. **C-D)** However, as the sequence of binding events was reversed and filamin was engaged with integrin before talin, the inhibited conformation of integrin was remained intact. The transparent regions of molecules were included in our model.

Tables:

Table 1

Interaction	Average Interaction Energy (kcal/mol)
Hydrophobic pocket - Ile ⁷⁵⁷ : Leu ²²⁷¹ and Phe ²²⁸⁵	-6.6 ± 1.1
Salt Bridge - Arg ⁷⁶⁰ : Asp ²²⁸⁷	-81 ± 10
Salt Bridge - Lys ⁷⁴⁸ : Glu ²²⁷⁶	-59 ± 31
Salt Bridge - Glu ⁷⁴⁹ : Lys ²²⁸⁰	-5.5 ± 6.2

Table 1 – The average interaction energies for specific residues important in the binding of integrin and filamin were calculated across ten extended trials of a successful bind in molecular dynamics simulations. This demonstrates that the strongest stable interaction is the salt bridge between Arg⁷⁶⁰ and Asp²²⁸⁷. The hydrophobic pocket insertion is weak because it is composed of Van der Waals forces, but it remains very stable. The salt bridge between Lys⁷⁴⁸ and Glu²²⁷⁶ is very unstable, appearing to switch between a low and a high energy state in all simulations, averaging in the end to a strength of -59 kcal/mol. The transient salt bridge that formed between Glu⁷⁴⁹ and Lys²²⁸⁰ within 2 ns and that disappeared by 5 ns, was indeed transient as its average interaction energy was negligible for an electrostatic interaction.

Figures:

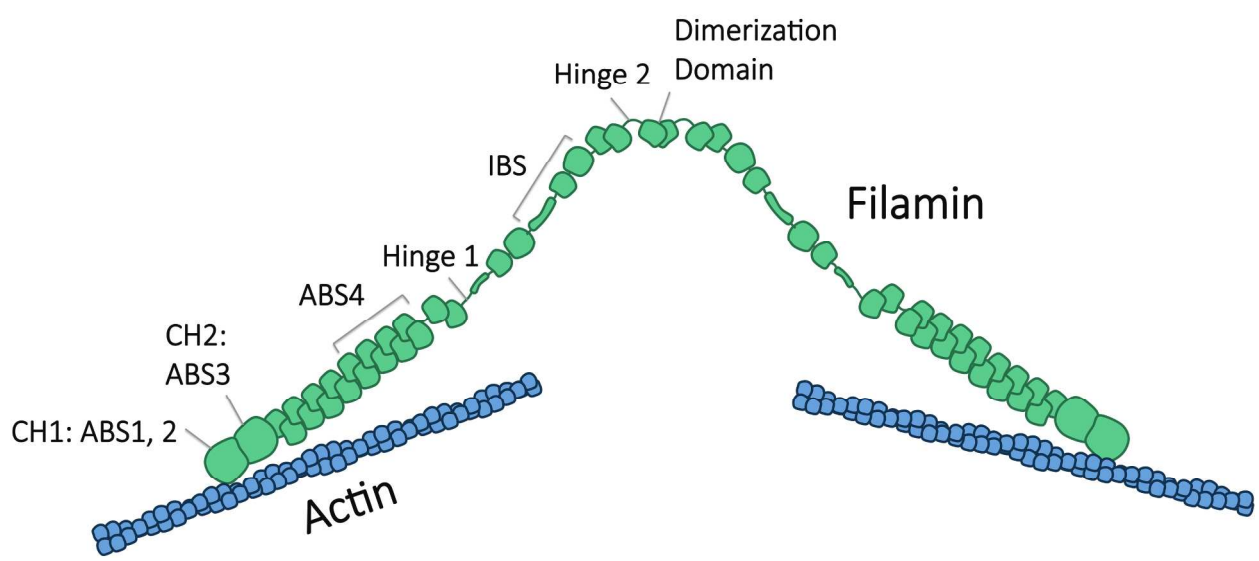


Figure 1

Integrative Biology Accepted Manuscript

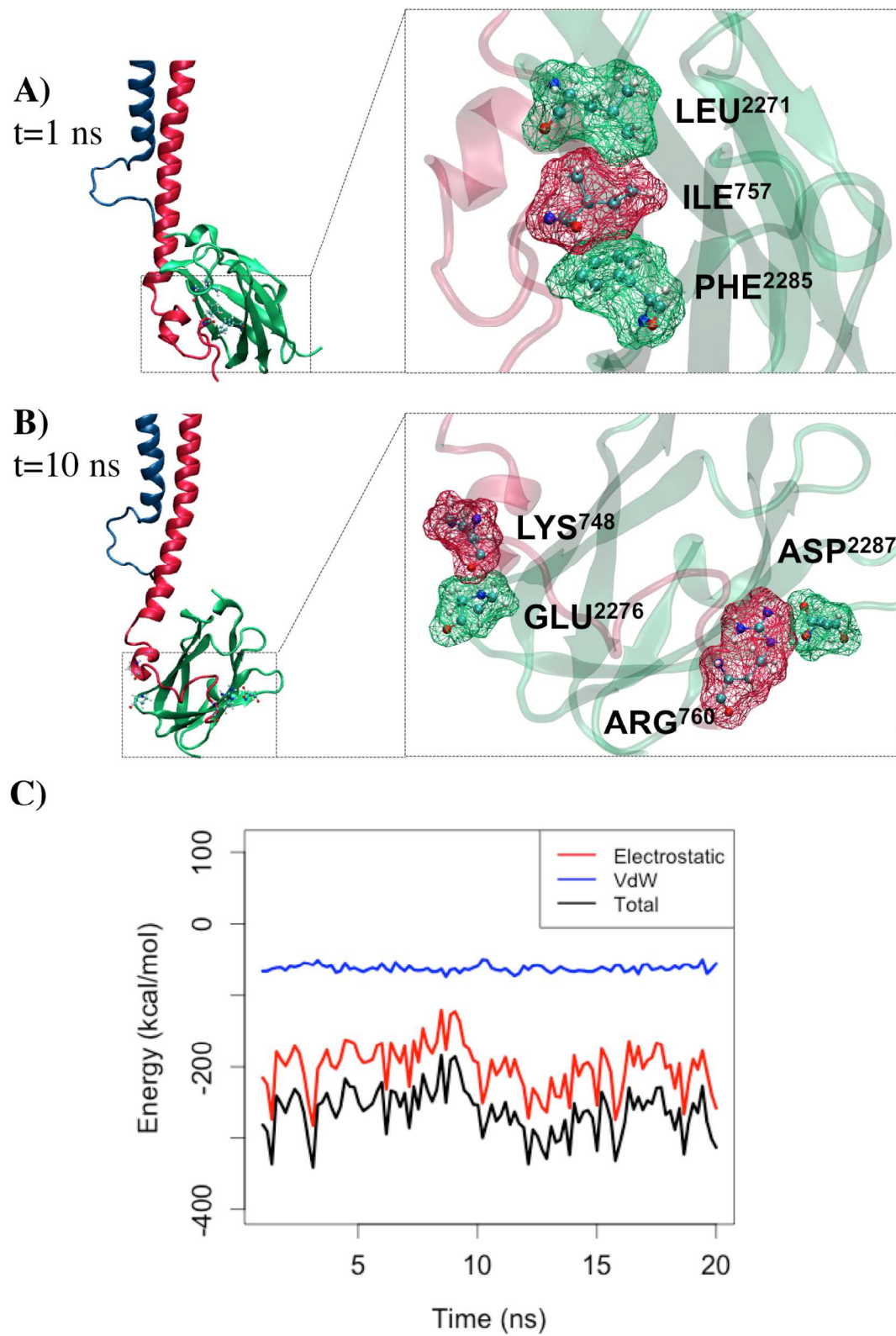


Figure 2

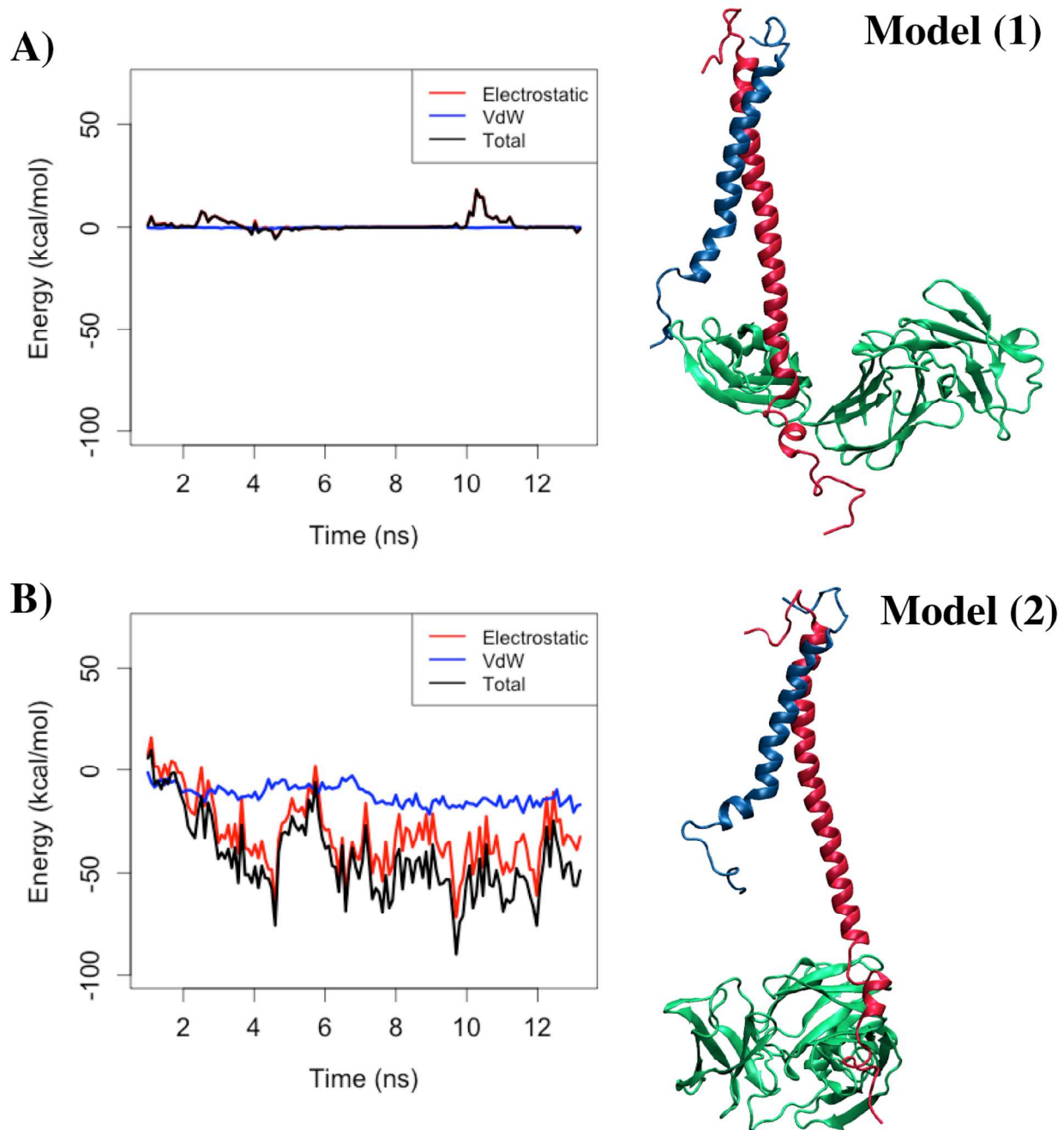


Figure 3

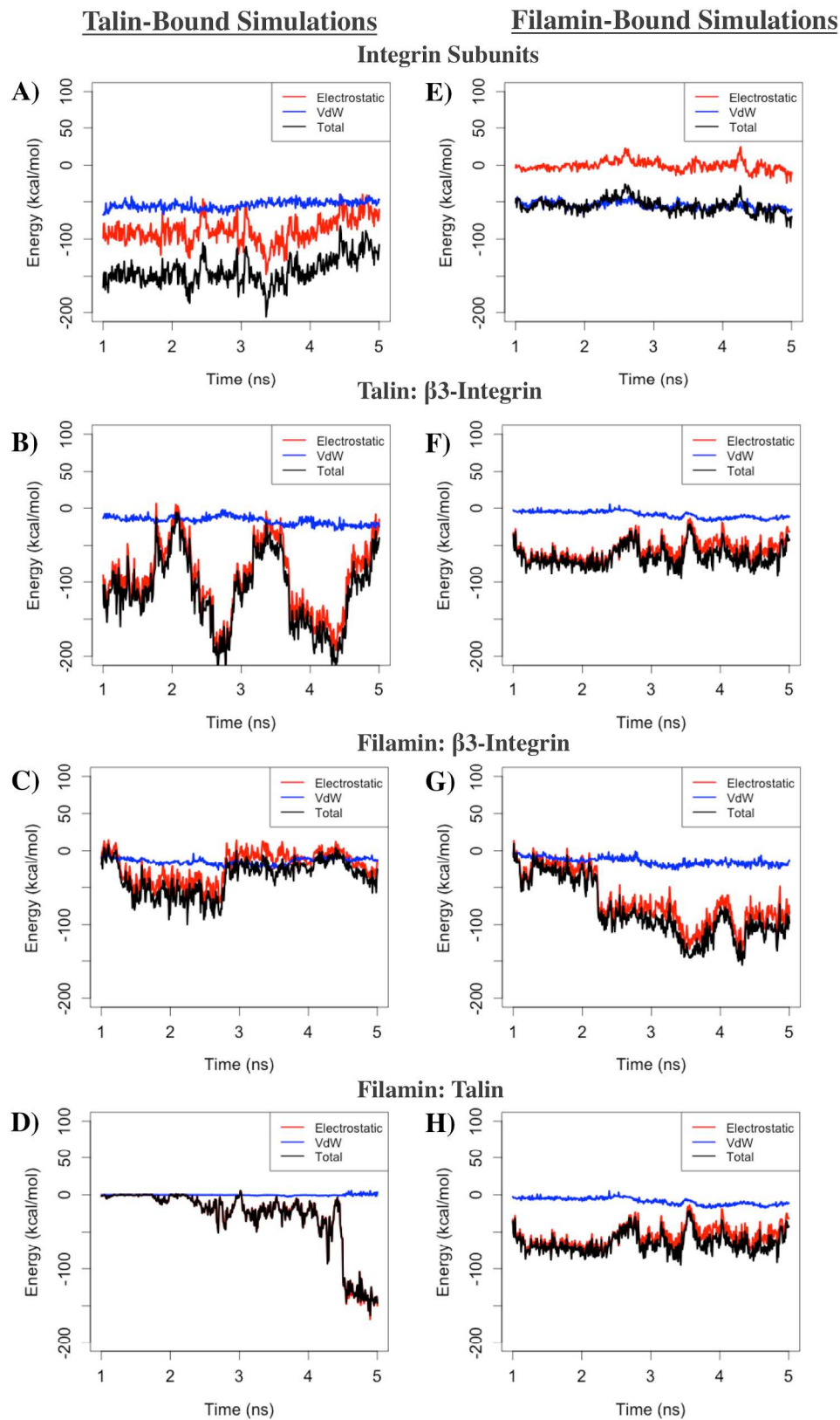


Figure 4

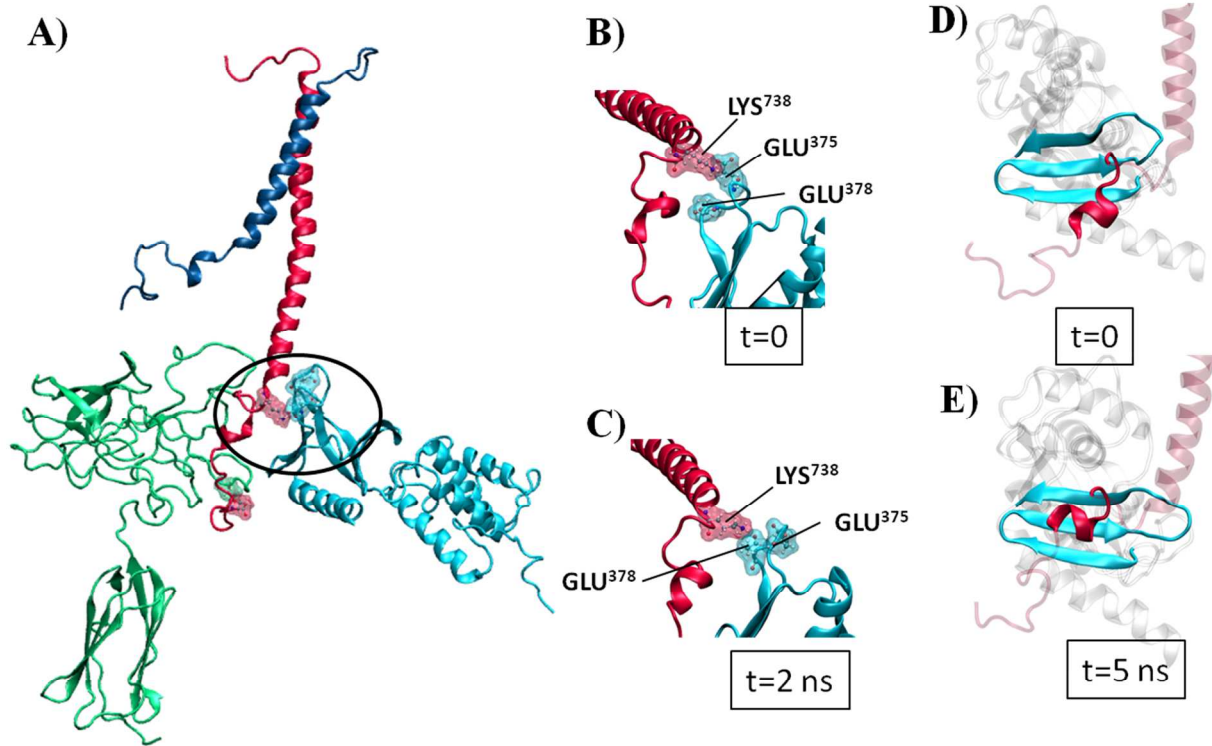


Figure 5

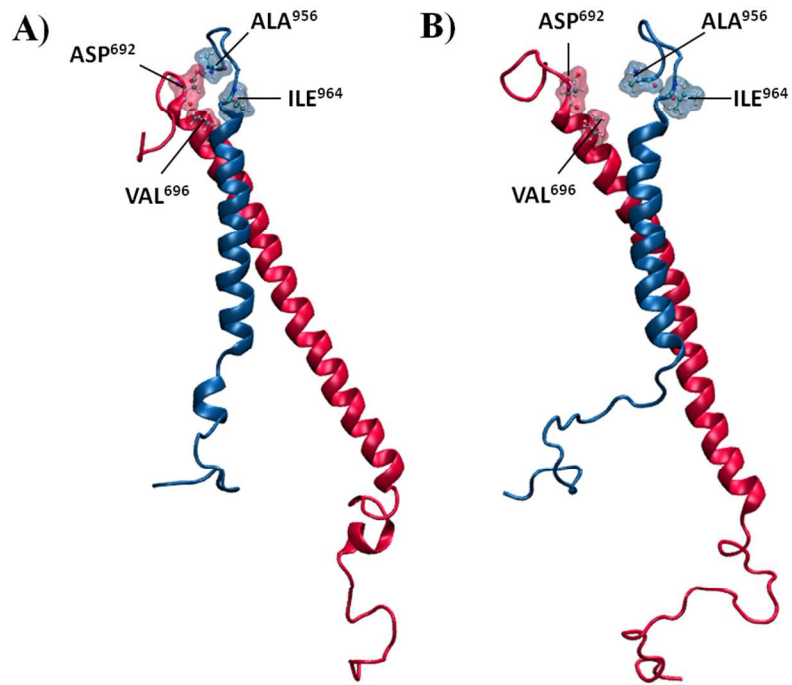


Figure 6

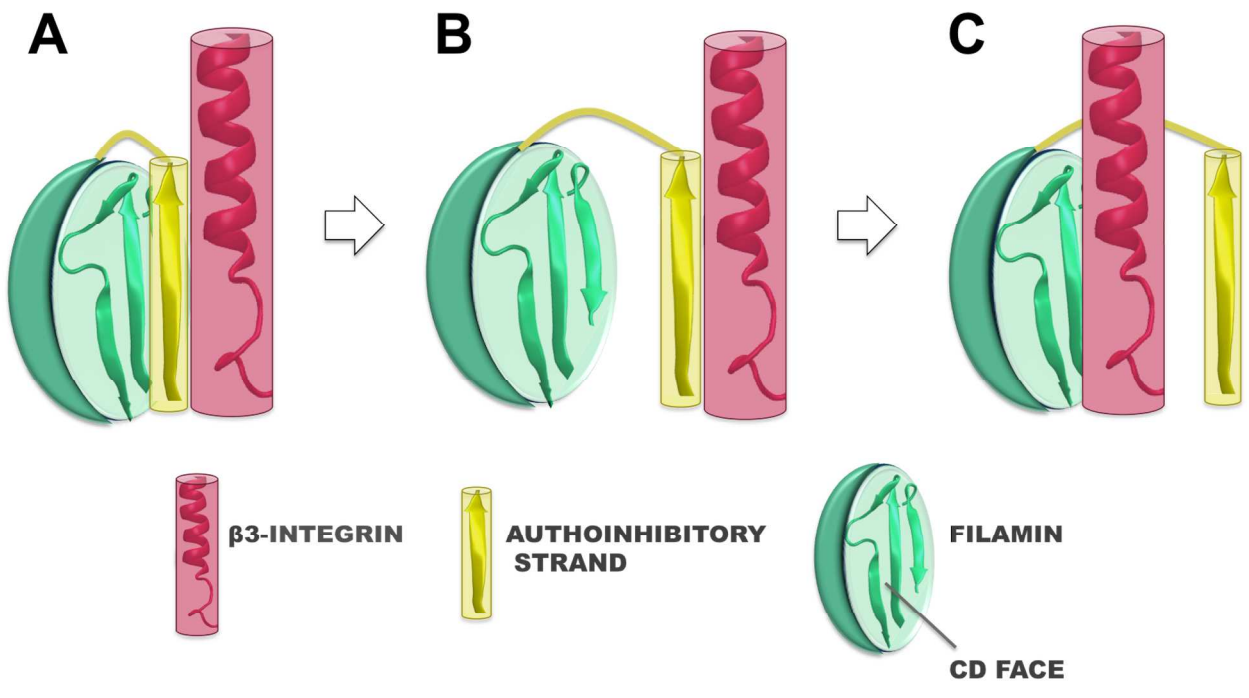


Figure 7

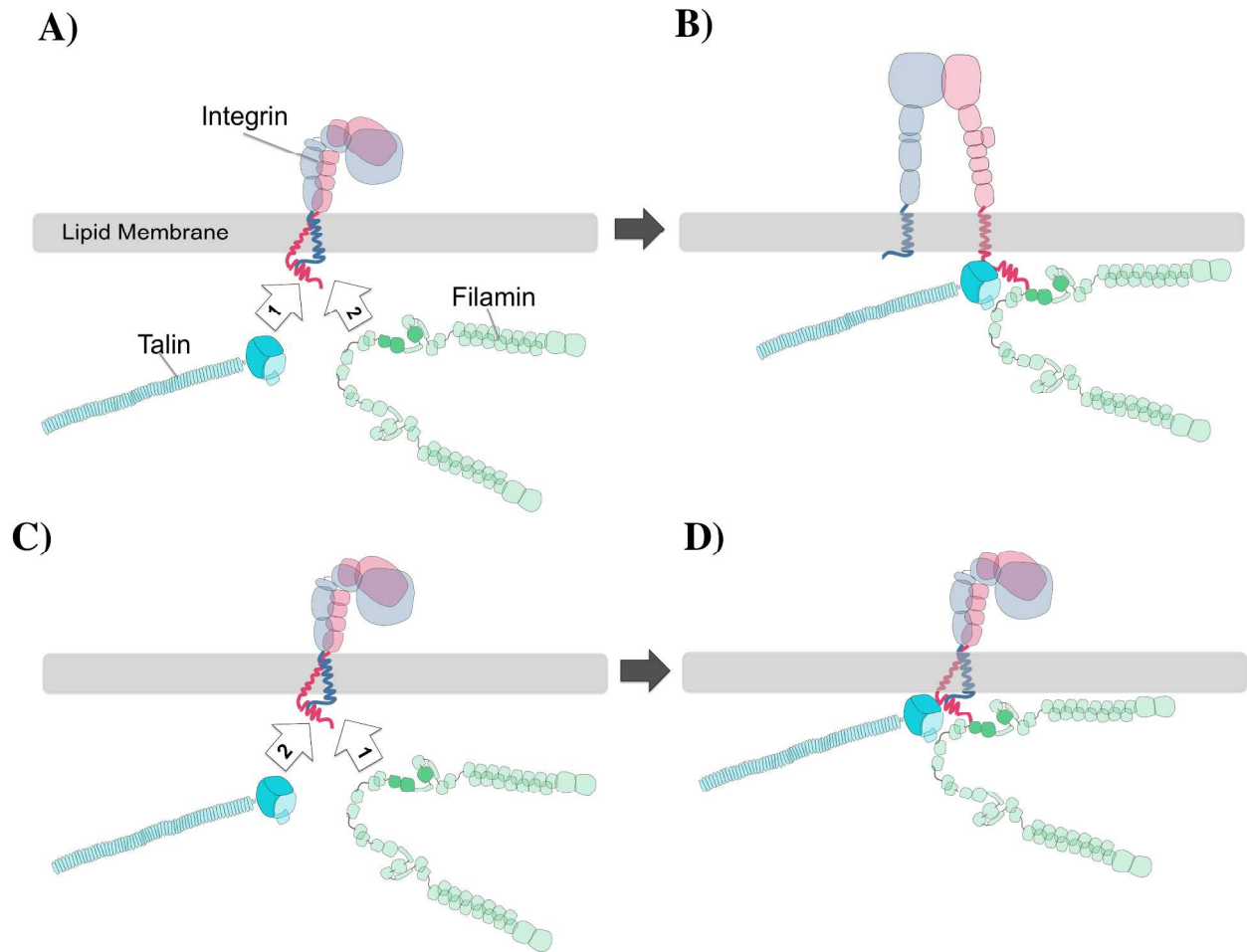


Figure 8